Heliyon 11 (2025) e42196

Contents lists available at ScienceDirect

Heliyon

journal homepage: www.cell.com/heliyon

Research article

High-fat diet triggers transcriptomic changes in the olfactory bulb

Young-Kook Kim [a,b,1], Danbi Jo [a,c,1], Seoyoon Choi [a,c], Juhyun Song [a,c,*]

[a] Biomedical Science Graduate Program (BMSGP), Chonnam National University, Hwasun, 58128, Republic of Korea
[b] Department of Biochemistry, Chonnam National University Medical School, Hwasun, 58128, Republic of Korea
[c] Department of Anatomy, Chonnam National University Medical School, Hwasun, 58128, Republic of Korea

ARTICLE INFO

Keywords:
Olfactory bulb
High-fat diet
RNA sequencing
Long non-coding RNA
Circular RNA

ABSTRACT

Metabolic imbalance contributes to cognitive impairment, anxiety, depressive behavior, and impaired olfactory perception. Recent studies have focused on olfactory dysfunction in patients with obesity and diabetes accompanied by cognitive dysfunction, considering that the synaptic signal from the olfactory bulb is directly transmitted to memory consolidation–related brain regions. This study investigated transcriptomic changes in the olfactory bulb in high-fat diet (HFD)-fed mice compared to that in normal-diet–fed mice. We sampled olfactory bulbs from HFD-fed mice, performed RNA sequencing, and measured mRNA levels in olfactory bulb tissue. Additionally, we assessed plasma cytokine levels in HFD-fed mice. We found differences in the expression of protein-coding and non-coding RNAs involved in insulin, lipid metabolism, neurogenesis, serotonin, dopamine, and gamma-aminobutyric acid–related signaling in the olfactory bulb of HFD-fed mice compared to control mice. Thus, our findings suggest potential therapeutic targets for treating olfactory dysfunction and related neural disorders in individuals with metabolic syndrome.

1. Introduction

Olfactory information influences eating behavior and neuronal circuit mechanisms associated with fear response, memory formation, depressive tendency, and social behavior in the central nervous system (CNS) [1,2]. Olfactory receptor neurons establish synaptic connections with the dendrites of mitral and tufted cells, serving as primary efferent projection neurons in the olfactory bulb, forming a synaptic relay structure (glomerulus) at the initial stage of smell perception [3]. In the olfactory bulb, the inhibitory synapses of mitral and tufted cells, alongside interneurons, undergo neuromodulation and play a crucial role in olfactory processing [4,5].

The olfactory bulb receives projection fibers from cholinergic, noradrenergic, serotonergic, and dopaminergic neurons [6–8]. Sensory olfactory information is conveyed from the olfactory epithelium to the olfactory bulbs through action potentials in olfactory receptor axons [9], subsequently projecting to various brain regions, including the piriform cortex, olfactory tubercle, anterior olfactory nucleus, entorhinal cortex, and amygdaloid body [10–12]. Then, neurons in these brain regions innervate the insular cortex, orbitofrontal cortex, and hippocampus [13].

Metabolic disorders disrupt neuronal synaptic function, compromising glucose metabolism and inducing insulin resistance in the olfactory bulb [14,15]. Obesity is characterized by alterations in hormone signaling and insulin receptor expression, contributing to

* Corresponding author. Department of Anatomy, Chonnam National University Medical School, Hwasun, 58128, Jeollanam-do, Republic of Korea.
E-mail address: juhyunsong@chonnam.ac.kr (J. Song).
[1] These authors contributed equally to this study.

https://doi.org/10.1016/j.heliyon.2025.e42196
Received 13 August 2024; Received in revised form 9 January 2025; Accepted 21 January 2025
Available online 22 January 2025

olfactory dysfunction [16–18]. A recent study has reported that short-term consumption of high-fat macronutrient food impairs odor behavior, brain metabolism, and brain synaptic connectivity [19–22].

Dysregulation of insulin-like growth factor 1 (IGF-1) diminishes olfactory sensitivity in individuals with obesity [23] and mice fed a high-fat diet (HFD) [24]. Additionally, an altered lipid profile is implicated in olfactory dysfunction among individuals with obesity [25,26]. Recent studies have indicated decreased olfactory function in individuals with obesity and diabetes, linking it to excessive adiposity and cognitive impairment [27–29]. Notably, patients with obesity commonly exhibit lower olfactory capacity [30], while HFD-fed mice demonstrate reduced olfactory discrimination and impaired odor-reversal learning due to the loss of olfactory sensory neurons [31].

RNA therapy has recently been investigated as a treatment for various diseases, being studied for its fast production speed and long-lasting effects. Particularly, non-coding RNAs are difficult to target with existing small molecule–based drugs but can be easily controlled using RNA-based molecules [32]. Recent studies have demonstrated the efficiency of intranasal RNA delivery in neurodegenerative diseases, such as age-related memory dysfunction and Alzheimer's disease, and neuropsychiatric diseases, including chronic anxiety [33,34]. Intranasal drug delivery targeting the olfactory bulb is a promising approach because the nose-to-brain pathway directly innervates various brain regions, including the hippocampus (which is related to cognition), the amygdala (which is related to mood behavior), and the hypothalamus (which is related to the autonomic nervous system), and is sensitive to changes in blood-brain barrier permeability [35–37]. Thus, RNA therapy holds promise as the treatment for neural diseases associated with olfactory dysfunction due to metabolic imbalance. Therefore, obtaining the expression profiles of non-coding RNAs and disease-related protein-coding RNAs, which expression is altered in certain diseases, and developing RNA therapeutics that target them are necessary.

This study aims to investigate the effects of the HFD on gene expression in the olfactory bulbs. We selected several protein-coding RNAs and non-coding RNAs, including long non-coding RNAs (lncRNAs) and circular RNAs (circRNAs), that are associated with olfactory dysfunction, neurotransmitter secretion, and metabolic imbalance in the olfactory bulb of HFD-fed mice. Additionally, this study assessed which cytokines are significantly altered in the blood plasma of HFD-treated mice. Here, we present the diverse effects of HFD on the expression of various genes in the olfactory bulb.

2. Materials and methods

2.1. Preparation of the mouse samples

Two-month-old male C57BL/6J mice were housed in the Laboratory Animal Research Center of Chonnam National University (CNU) under a 16-h light/8-h dark cycle at 23 °C with 60 % humidity. We used only male mice in this experiment because feeding an HFD to male mice induces more fat mass and metabolic disorder; thus, male mice are more susceptible to obesity and hyperinsulinism [38,39]. The normal-fat diet (NFD; 22 kcal% fat, 22 kcal% carbohydrate, and 56 kcal% protein, purchased from DBL, Korea, RodFeed) and high-fat diet (HFD; 45 kcal% fat, 35 kcal% carbohydrate, and 20 kcal% protein, purchased from Research Diets, USA, D12451) mice were given *ad libitum* access to food and water during the experiment. Two-month-old mice were fed a diet for 4 months, with 3 mice per group. After 4 months of HFD, 3 mice per group (NFD and HFD groups) were anesthetized and sacrificed by cervical dislocation in the morning. Afterward, their brains were isolated for total RNA sequencing (RNA-seq), semi-quantitative polymerase chain reaction (PCR), and real-time PCR.

Mice plasma samples were used for cytokine array, whereas brain tissue samples were used for total RNA-seq analysis, semi-quantitative PCR, and real-time PCR. Due to the limited number of animals used in this study, randomization was not performed during group allocation. The experimenters who conducted the experiments also performed data analysis without blinding, following standardized protocols to ensure objective and reliable evaluation. The experiments were performed following the recommendations of the 96 guidelines for animal experiments established by the Animal Ethics Committee at the CNU (CNU IACUC-H-2022-8). The Animal Ethics Committee at the CNU approved the respective protocol.

2.2. RNA sequencing analysis

RNA samples from each NFD- or HFD-fed mouse's olfactory bulb were prepared for RNA-seq analysis. Total RNA was extracted using an RNAiso Plus (Takara, Japan), with integrity identified using a 2100 bioanalyzer system (Agilent). RNA-seq libraries were prepared using the TruSeq Stranded Total RNA kit (Illumina) and the NovaSeq 6000 system (Illumina).

Following sequencing, the reads with low quality were removed or trimmed using Trimmomatic [40]. The remaining sequences were aligned to the mouse genome (mm10) using the spliced transcripts alignment to a reference (STAR) [41]. The normalized values of the fragments per kilobase of transcript per million mapped reads (FPKMs) were calculated using Cuffnorm based on the GENCODE annotation (Release M23, GRCm38.p6) [42]. The genes with an average FPKM of <1 or those not detected in any samples were excluded from further analysis. Genes showing significant differences between NFD and HFD groups were selected by *t*-test analysis based on FPKM values.

Then, we analyzed RNA-seq results again with a different kind of algorithm to further increase the reliability of our results [43]. Using the FASTQ reads after filtering out low-quality reads with Trimmomatic, the transcript level of each gene was counted using the Salmon algorithm based on the GENCODE annotation used before [44]. The fold ratio, *p*-value, and false discovery rate of each gene were calculated using the edgeR [45]. Supplementary Table S1 presents the analysis results.

We selected the gene class of "lncRNA" as annotated in the GENCODE to analyze long non-coding RNA (lncRNA) expression. The DCC algorithm was used to measure the reads from the back-splicing junction to analyze the expression of circular RNAs (circRNAs)

[46]. We only used the circRNA loci with average expression counts of >5 after normalization for further analysis.

2.3. Genes with altered expression

We selected a list of genes with significantly changed expression with a p-value <0.05 across both algorithms (STAR-Cuffnorm and Salmon-edgeR) to select genes with significant expression changes in the olfactory bulb from HFD-fed mice compared to NFD-fed mice. This list included 211 genes with decreased expression and 89 genes with increased expression, which were used for functional analysis. Based on this group of genes, Gene Ontology (GO) analysis was performed using the Molecular Signatures Database [47]. Afterward, the 15 most important detected GO terms were selected based on the FDR q-value.

2.4. Measurement of RNA expression

Total RNA was isolated from mouse olfactory bulbs using RNAiso Plus (Takara) according to the manufacturer's instructions. Two μg of extracted total RNA was reverse transcribed to complementary DNA (cDNA) using a random hexamer (Thermo Fisher Scientific, USA) and RevertAid reverse transcriptase (Thermo Fisher Scientific). Quantitative real-time PCR (qRT-PCR) based on the comparative Ct method was performed using the Power SYBR Green PCR master mix (Applied Biosystems, USA) and the Step One Plus real-time PCR system (Applied Biosystems). qRT-PCR reactions were conducted at 95 °C for 10 min, followed by 40 cycles of 95 °C for 15 s and 60 °C for 1 min. Finally, the reaction was completed after cycles for 15 s at 95 °C, 1 min at 60 °C, and 15 s at 95 °C.

Semi-quantitative PCR was conducted using nTaq DNA polymerase (Enzynomics, Korea) and Phusion DNA polymerase (Thermo Fisher Scientific) in the Master cycler Nexus X2 (Eppendorf, Germany), before confirming by 2 % agarose gel electrophoresis and quantifying with Image J software (ver. 1.52), to measure circRNA expression. The semi-quantitative PCR reactions of *circAPP*, *circTRPC6*, and *GAPDH* were performed with 20 ng of cDNA. *circAPP* was performed using phusion DNA polymerase at 98 °C for 30 s, followed by 30 cycles of 98 °C for 10 s, 63 °C for 30 s, 72 °C for 1 min, and 72 °C for 5 min *circTRPC6* was performed at 95 °C for 2 min, followed by 30 cycles of 95 °C for 30 s, 61 °C for 30 s, 72 °C for 30 s, and 72 °C for 5 min using nTaq DNA polymerase. *GAPDH* was performed at 95 °C for 2 min, followed by 23 cycles of 95 °C for 30 s, 61 °C for 30 s, 72 °C for 30 s, and 72 °C for 5 min using nTaq DNA polymerase. First-strand cDNA was synthesized using the miRCURY LNA RT Kit (QIAGEN, Germany) in the Master cycler Nexus X2 according to the manufacturer's instructions to identify microRNA (miRNA) expression. miRNA was detected using the miRCURY LNA SYBR Green PCR Kit (QIAGEN) according to the manufacturer's instruction in the Step One Plus real-time PCR system. The expression level of miRNAs was normalized to U6 snRNA (v2). The PCR primers for miR-124-3p, miR-325-3p, and U6 snRNA were purchased from QIAGEN. The expression of circRNA or mRNA was normalized to the expression of *GAPDH*. qRT-PCR reactions were conducted at 95 °C for 2 min, followed by 40 cycles of 95 °C for 10 s and 56 °C for 1 min. Finally, the reaction was completed after cycles for 15 s at 95 °C, 1 min at 60 °C, and 15 s at 95 °C. Table 2 provides the list of all primer sequences.

2.5. Cytokine array

The cytokine array (R&D system, ARY022B, USA) was performed according to the manufacturer's instructions. Mice's plasma was isolated by centrifuging at 4 °C and 10,000 rpm for 10 min. The membrane for the cytokine array was incubated in a blocking solution for 1 h at room temperature, followed by incubation with mouse plasma samples for 16 h at 4 °C. Subsequently, the membranes were washed three times and incubated with a detection antibody cocktail for 1 h at room temperature. Then, the membranes were incubated with 1X Streptavidin-HRP at room temperature for 30 min. The membranes were visualized using Chemi Reagent Mix and Fusion Solo software (16.0.8.0).

The plasma mixture from 3 NFD-fed mice was collected into one tube, while that from 3 HFD-fed mice was collected into another tube to prepare samples for this experiment. The same plasma mixtures were measured twice with two membranes, respectively. Each membrane contained 2 dots for each protein, making 4 data points for each protein. Cytokines and chemokines with statistically significant changes between NFD and HFD groups were represented in the graph (n = 3). Each point was normalized to the reference point. Furthermore, data were presented as the mean ± standard error of the mean (SEM).

2.6. Statistical analysis

All data were analyzed using unpaired two-tailed t-tests with Welch's correction between groups. Statistical analysis was conducted using GraphPad Prism (8.0). Data are represented as the mean ± standard error of the mean (SEM). For expression confirmation experiments (n = 3 per group), a one-sided Mann-Whitney U test was used to detect directional differences between groups. For the cytokine array experiment (n = 4 per group), a two-sided Mann-Whitney U test was applied to assess differences in either direction. Data were considered significant at $*p < 0.05$, $**p < 0.01$, $***p < 0.005$, and $****p < 0.001$.

3. Results

3.1. Transcriptome analysis in the olfactory bulbs of HFD-fed mice

HFD-fed mice were used in our investigation of olfactory dysfunction influenced by a metabolic imbalance. After feeding two-week-old mice a high-fat diet (HFD) for 4 months, all mice were sacrificed, and brain cortex was collected for transcriptome analysis. When

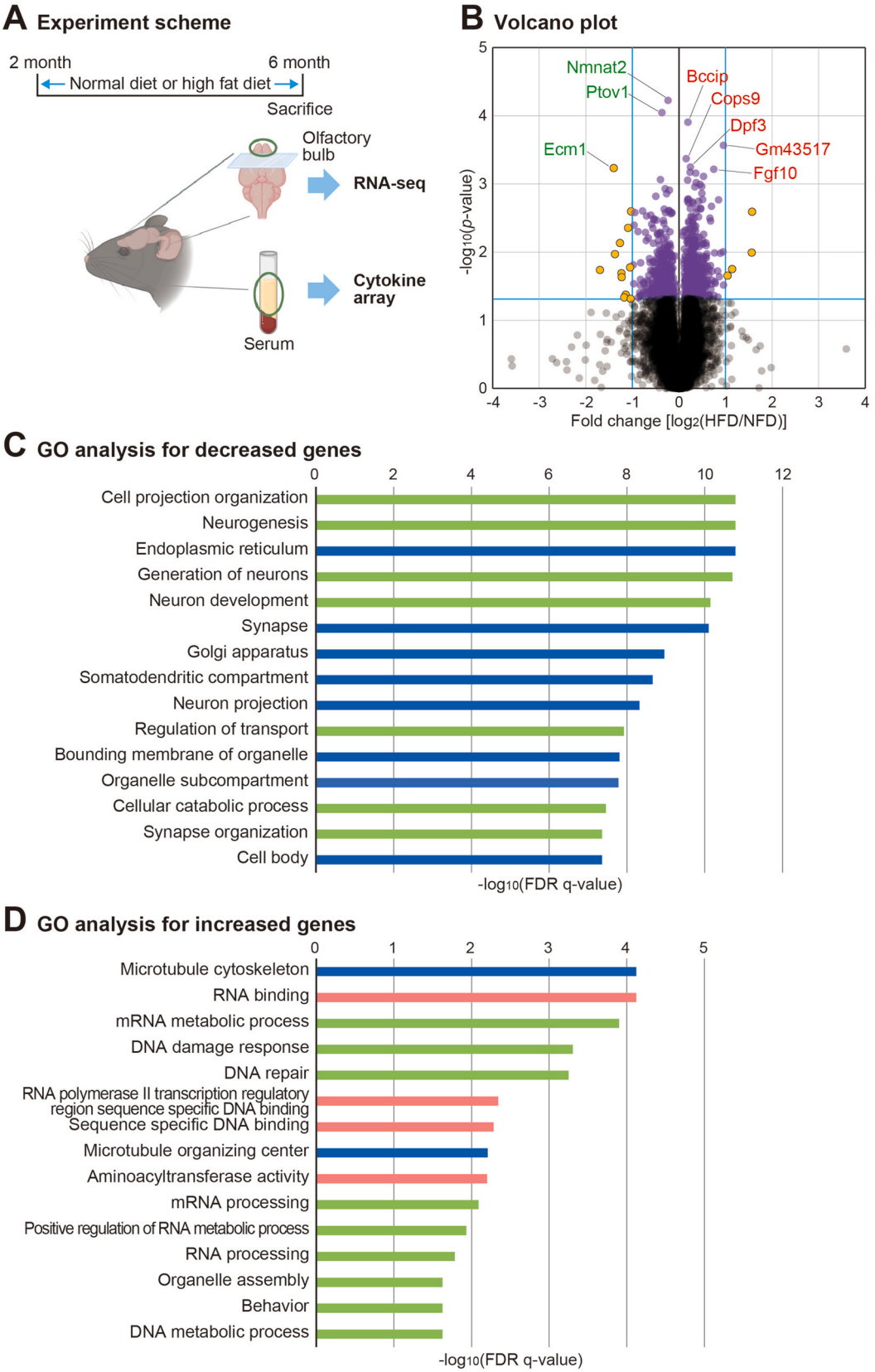

(caption on next page)

Fig. 1. Transcriptome analysis in the olfactory bulbs of mice fed a high-fat diet. (A) Experimental scheme of this study. After feeding two-week-old mice a high-fat diet (HFD) for 4 months, all mice were sacrificed, and brain cortex was collected for transcriptome analysis. When mice were sacrificed, serum was collected and cytokine array was performed. Brain cortex and serum from three mice in the normal fat diet (NFD) group and three mice in the HFD group were collected for experiments, respectively. The image was created by using Biorender. (B) Volcano plot. The volcano plot was drawn based on the gene expression change data obtained from the transcriptome analysis results. The blue vertical and horizontal lines represent points with a $\log_2$(fold change) of 2 and a *p-value* of 0.05, respectively. The names of the genes with the most significant expression changes are indicated based on *p*-value. Red colored genes indicate upregulated genes ($\log_2$(HFD/NFD) > 0), whereas green colored genes indicate downregulated genes ($\log_2$(HFD/NFD) < 0). The genes marked with yellow and purple dots were used for the gene ontology (GO) analysis below. (C) GO analysis for decreased genes. For the 211 downregulated genes with *p*-values <0.05 in both algorithms (see Method 2.2), GO term analysis was performed. The 15 most significant GO terms, determined based on the false discovery rate (q-value), are presented. (D) GO analysis for increased genes. For the 89 upregulated genes with *p*-values <0.05 in both algorithms, GO term analysis was performed and shown in the same way as in (C). In (C) and (D), the bars with blue, green, and red colors indicate the GO term domains with cellular component, biological process, and molecular function, respectively. NFD: normal fat diet, HFD: high fat diet.

mice were sacrificed, serum was collected and cytokine array was performed. Brain cortex and serum from three mice in the normal fat diet (NFD) group and three mice in the HFD group were collected for experiments, respectively (Fig. 1A). Plasma samples were collected to assess the expressions of cytokines and adipokines in all mice. A comprehensive comparison of the transcriptome profiles in the olfactory bulbs of HFD- and NFD-fed mice was conducted through RNA-seq analysis (see Method 2.2; Supplementary Table S1). The resulting volcano plot represents a variety of differentially expressed genes in the olfactory bulb following HFD (Fig. 1B). Several genes involved in metabolic diseases and neural signaling, including *FGF10*, *ECM1*, and *NMNAT2*, showed significant expression changes in the olfactory bulbs of HFD-fed mice.

Subsequently, gene ontology (GO) analysis was performed on significantly down- and upregulated genes, and the 15 most significant detected GO terms were selected for each group (Fig. 1C and D). The GO analysis of downregulated genes revealed an abundance of GO terms related to neurogenesis, neuronal function, neuronal development, and synapse-related processes (Fig. 1C). Conversely, the GO analysis of upregulated genes demonstrated significant enrichment in GO terms linked to RNA biogenesis and function, such as RNA binding and RNA processing (Fig. 1D).

3.2. Analysis of expression changes in metabolic and neural signaling-related genes and cytokine in HFD-fed mice

The HFD-induced metabolic changes may influence signaling pathways associated with metabolic and neurosignaling-related genes in olfactory neurons. This possibility was further suggested by the GO term analysis. Thus, we examined the expression changes of genes implicated in these signaling pathways using RNA-seq results. Specifically, we verified changes in the mRNA level of genes associated with fatty acid (*FFAR1*, *FFAR4*, and *PDK4*), insulin (*IRS2, SLC2A1, SLC2A4*, and *SLC2A5*), neurogenesis (*NTRK2* and *SCN1B*), and dopamine receptors (*DRD1* and *DRD2*) in the olfactory bulb of HFD-fed mice (Fig. 2A).

We found that reduced mRNA level of fatty acid related genes such as *Ffar1, Ffar4* and *Pdk4* in the olfactory bulbs of HFD mice compared to those of normal mice (Fig. 2A). We observed that decreased mRNA level of insulin-related genes including *Irs2, Slc2a1, Slc2a4* and *Slc2a5* in the olfactory bulb of HFD mice compared to those of normal mice (Fig. 2A). Also, we found the reduced mRNA levels of neurogenesis related genes such as Ntk2 and Scn1b in the olfactory bulb of HFD mice compared to those of normal mice (Fig. 2A). Conversely, we found the increased mRNA levels of dopamine receptor Drd1 and Drd2 in the olfactory bulb of HFD mice compared to those of normal mice (Fig. 2A). In olfactory bulb neurons, the HFD reduced the expression of genes related to Ffar1 signaling involved in insulin secretion by enhancing mitochondrial respiration [48], Ffar4 signaling involved in polyunsaturated fatty acid metabolism [49], insulin signaling, and neurogenesis while concurrently increasing the expression of dopamine receptor genes. Furthermore, the expression of several members of gene families, including those related to insulin, serotonin, glucose, and GABA receptors, was changed in the olfactory bulb of HFD fed mice (Supplementary Fig. S1).

We examined different levels of cytokines between NFD mice plasma and HFD mice plasma to explore the relationship between HFD-induced transcriptomic changes in the olfactory bulb and cytokine levels in plasma. Using cytokine array experiments, we determined that several cytokines involved in the immune response, metabolism, and cell growth, including cluster of differentiation 14 (CD14), chemerin, epidermal growth factor (EGF), insulin-like growth factor-binding protein 1 (IGFBP-1), and matrix metalloproteinase-2 (MMP2), were reduced in the plasma of HFD-fed mice (Fig. 2B). In contrast, endoglin (CD105), as angiogenesis-related membrane glycoprotein, and pro-inflammatory hormones, including leptin, were increased in the plasma of HFD-fed mice (Fig. 2B). Therefore, an HFD reduces cellular signaling related to the suppression of cell growth, immune response, and metabolism while concurrently increasing cellular signaling associated with inflammation, indicating a potential impact on diverse signaling pathways.

3.3. Analysis of the expression and possible regulatory mechanism of differentially expressed long non-coding RNAs (lncRNAs) in the olfactory bulb of mice fed a high-fat diet

After the GO analysis of the upregulated genes, we observed a significant enriched GO terms related to RNA binding and RNA processing (Fig. 1D). Subsequently, our focus shifted to identifying changes in non-coding RNA expressions. Specifically, we investigated changes in lncRNAs and circRNAs, which have been extensively investigated in recent years. Fig. 3A shows the lncRNAs with significant changes in the olfactory bulb of HFD-fed mice compared to NFD-fed mice (Fig. 3A). We found the significantly changed

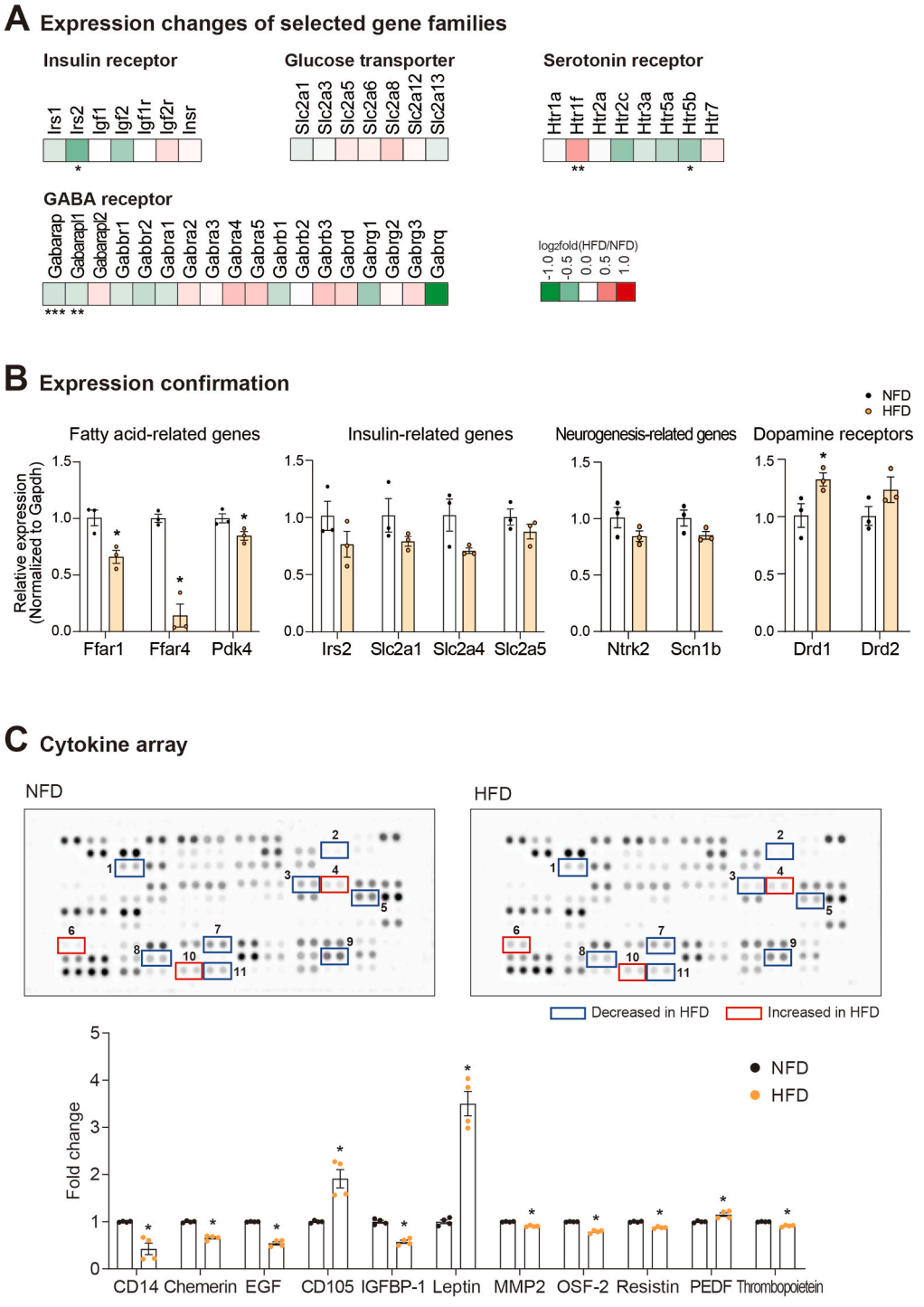

Fig. 2. Analysis of expression changes in metabolic and neural signaling-related genes and cytokines in mice fed a high-fat diet. (A) quantitative real-time polymerase chain reaction (qRT-PCR) measurement of fatty acid, insulin, neurogenesis, and dopamine receptor–related genes in the olfactory bulb of normal-fat diet (NFD) and high-fat diet (HFD)-fed mice. mRNA expression was normalized to *GAPDH*. Data are represented as the mean ± standard error of the mean (SEM; $n = 3$). Statistical analyses were performed using a one-sided Mann-Whitney *U* test (Ffar1: $p = 0.05$; Ffar4: $p = 0.05$; Pdk4: $p = 0.05$; Irs2: $p = 0.2$; Slc2a1: $p = 0.1$; Slc2a4: $p = 0.1$; Slc2a5: $p = 0.2$; Ntrk2: $p = 0.1$; Scn1b: $p = 0.1$; Drd1: $p = 0.05$; Drd2: $p = 0.2$; $^*p < 0.05$). (B) A cytokine array was performed to measure cytokine levels in the plasma of mice. For each group (NFD and HFD), plasma was collected from three mice and pooled into a single sample. This pooled plasma was then used to assess cytokine and chemokine expression using the cytokine array kit. To ensure reliability, the same pooled plasma sample was analyzed twice using two separate membranes. Each membrane contained duplicate spots for each protein, resulting in a total of four data points per protein (two spots per membrane × two membranes). The

cytokines with significant differences between NFD- and HFD-fed mice groups are labeled with Arabic numerals, with blue boxes indicating decreased cytokine levels and red boxes indicating increased cytokine levels in HFD-fed mice compared to NFD-fed mice. Data are presented as the mean ± SEM ($n = 4$). Statistical analyses were performed using a two-sided Mann-Whitney U test (CD14: $p = 0.0286$; chemerin: $p = 0.0286$; EGF: $p = 0.0286$; CD105: $p = 0.0286$; IGFBP-1: $p = 0.0286$; leptin: $p = 0.0286$; MMP2: $p = 0.0286$; OSF-2: $p = 0.0286$; resistin: $p = 0.0286$; PEDF: $p = 0.0286$; thrombopoietin: $p = 0.0286$; *$p < 0.05$). NFD: normal fat diet, HFD: high fat diet.

lncRNAs including Gm19744, Gm29521, Gm44763, Gm27032, Airn, Ftx, A830036E02Rik, 9530059O14Rik, E130307a14Rik, A330076H08Rik,5330434G04Rik, and Dlx6os1 (Fig. 3A). Next, we examined the genomic loci of these differentially expressed lncRNAs, showing that the loci of many lncRNAs overlapped with the position of mature miRNA sequences on the genome (Fig. 3B). Fig. 3B reveals genomic locus of miRNA-hosting lncRNAs such as A330076H08Rik, 9530059O14Rik, Gm27032, 5330434G04Rik and Ftx (Fig. 3B).

Given that miRNAs are generated from longer primary transcripts containing stem-loop structures (primary miRNAs; pri-miRNAs), with many lncRNAs producing pri-miRNAs, a potential correlation between miRNAs and lncRNAs they originate from was hypothesized [50]. Therefore, we selected miR-124 and miR-325, derived from Gm27032 and 5330434G04Rik, respectively, measuring their expression in the tested samples. Contrary to our expectations, miR-124-3p and miR-325-3p were significantly downregulated in the olfactory bulb of HFD-fed mice (Fig. 3C). The observed increase in primary miRNAs and decrease in mature miRNA products suggests a potential impact on miRNA processing enzymes during the miRNA biogenesis pathway. Upon examining the expression levels of biogenesis factors from the RNA-seq data, we noted a slight increase in Dgcr8 and Tarbp2, which are RNA binding proteins in the miRNA biogenesis pathway, in the olfactory bulb of HFD-fed mice (Supplementary Fig. S2). However, it remains uncertain whether changes in the expression of these genes translate to changes in protein levels, subsequently impacting miRNA production. Therefore, further investigations are warranted to address this question since the miRNA expression changes we observed might not relate to the control of factors involved in miRNA production.

3.4. Analysis of the expression changes in selected circRNAs and their relationship with their host genes

Recent investigations have highlighted variations in the expression of circRNAs across diverse diseases [51,52]. We systematically computed the expression of circRNAs from the RNA-seq data since changes in RNA binding or RNA processing in the olfactory bulb of HFD-fed mice, as indicated by the GO analysis (Fig. 1D), may influence circRNA expression. Then, we conducted a comparative analysis of circRNA expression differences in the olfactory bulb of NFD-versus HFD-fed mice (Table 1 and Fig. 4A).

Among circRNAs displaying significant expression changes in RNA-seq, we specifically assessed the expression of circApp and circTrpc6, based on whether the host gene of circRNA is involved in neural function. Previous reports implicated App and Trpc6, the host mRNAs of circApp and circTrpc6, respectively, in neuron-related functions, including memory formation and synaptic plasticity [53,54]. Our findings confirmed reduced circApp expression and increased circTrpc6 expression in the olfactory bulb of HFD-fed mice (Fig. 4B). We investigated the correlation between the expression of these circRNAs and their corresponding host mRNAs (Fig. 4C). Our results demonstrated a clear positive correlation in the expression of both App mRNA-circApp and Trpc6 mRNA-circTrpb6 pairs, suggesting that as the expression of the host genes increases, so does the production of circRNAs from them (Fig. 4D). A previous report found that human APP mRNA (circ3323)-derived circRNA promotes the expression of the host gene by suppressing miR-186-5p [55]. However, no study has yet suggested any mechanistic insight into the correlation between circTrpc6 and its host gene. Thus, a more comprehensive investigation is imperative to identify a functional link between these proteins and circRNA pairs to substantiate our claim.

4. Discussion

Since obesity is accompanied by olfactory dysfunction, we investigated the transcriptomic changes in the olfactory bulb of HFD-fed mice compared to the olfactory bulb of NFD-fed mice and searched for significantly changed genes involved in olfactory dysfunction. We identified various protein-coding, lncRNAs, and circRNAs, which expression was changed in the olfactory bulb of HFD-fed mice. Furthermore, we found that several cytokines related to immune response, metabolism, and cell growth were changed in the plasma of HFD-fed mice. Our investigation centered on assessing olfactory dysfunction and identifying significantly related coding- and non-coding RNAs in the olfactory bulb of HFD-fed mice.

Fig. 1B illustrates distinct genes identified in the olfactory bulbs of HFD-fed mice, showcasing notably increased genes, such as *FGF10*. *FGF10*, expressed in neurogenic niches, is linked to the negative control of neurogenesis, suggesting that HFD may decrease neurogenesis in the olfactory bulb [56,57]. Conversely, *ECM1* and *NMNAT2* expression was significantly decreased in the olfactory bulbs of HFD-fed mice. Reduced *ECM* expression may be linked to diminished neuroblast migration into the olfactory bulb [58,59]. Moreover, reduced *NMNAT2* expression suggests that HFD could influence axonal trafficking and neurite outgrowth in the olfactory bulb [60,61]. Moreover, the roles of *GM43517, DPF3, COPS9, BCCIP*, and *PTOV1* genes need to be investigated in the olfactory bulb in obesity.

Cell projection organization and neurogenesis, representing enriched terms from GO analysis (Fig. 1C), are pivotal in the olfactory bulb under stress [62]. Previous studies reported that HFD induces olfactory sensory neuronal loss, impairs axonal projection, and affects adult neurogenesis [14,20,31,63]. Our data suggested that HFD impairs neurogenesis, synapse, and axonal projection and triggers olfactory sensory neuronal cell loss in the olfactory bulb.

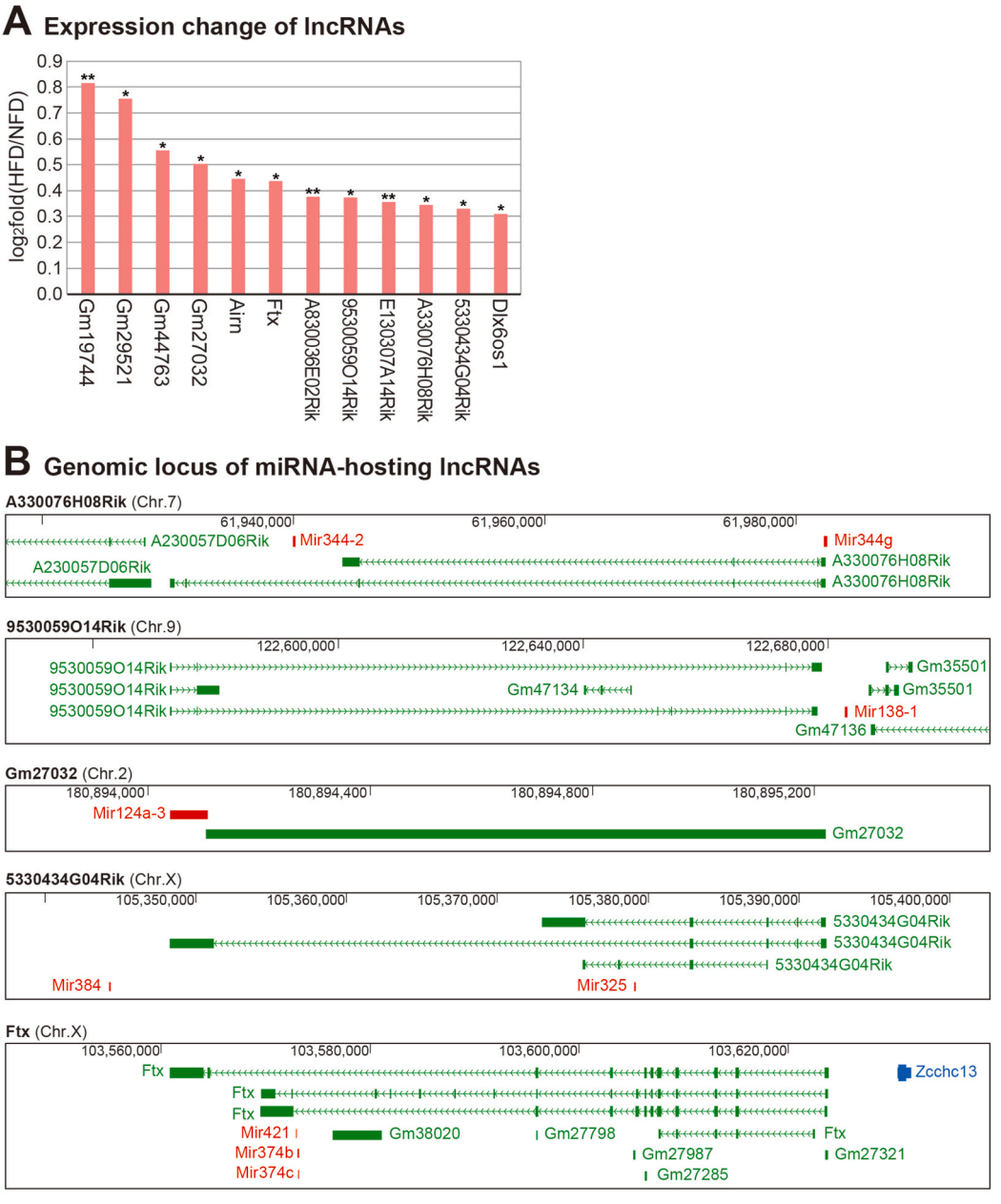

(caption on next page)

Fig. 3. Analysis of the expression and possible regulatory mechanism of differentially expressed long non-coding RNAs (lncRNAs) in the olfactory bulb of mice fed a high-fat diet. (A) Expression change of lncRNAs. The expression of lncRNAs ($p < 0.05$) in the olfactory bulb of mice on a high-fat diet that was most significantly changed compared to mice on a normal diet is presented in log2fold order (*$p < 0.05$, **$p < 0.01$). (B) Genomic locus of miRNA-hosting lncRNAs. Among the lncRNAs presented in (A), in cases when miRNAs were present at a position in the genome that overlapped with the sequence of the lncRNA, the relative position of the miRNA on the genome was indicated with the lncRNA. The location information on the genome was obtained from the UCSC Genome Browser (https://genome.ucsc.edu/). (C) Expression confirmation of selected miRNAs. The expressions of miR-124-3p and miR-325-3p were measured using quantitative real-time polymerase chain reaction (qRT-PCR). miRNA expression was normalized to U6 snRNA. Data are presented as the mean ± standard error of the mean (SEM; $n = 3$). Statistical analyses were performed using a one-sided Mann-Whitney *U* test (miR-124-3p: $p = 0.05$; miR-325-3p: $p = 0.05$; *$p < 0.05$). NFD: normal fat diet, HFD: high fat diet, r: Pearson correlation coefficient.

Upon measuring the mRNA levels of neurotransmitter receptors by RT-PCR, we observed decreased Ntrk2b expression and increased Drd1 and Drd2 expression in the olfactory bulbs of HFD-fed mice (Fig. 2A). The neurotrophin receptor Ntrk2b plays a pivotal role in sustaining dopamine and serotonin neuronal function [64]. Additionally, BDNF/NTRK2 signaling is involved in the pathophysiology of depression [65,66] and the reward system through the dopaminergic circuit [66,67]. Our data indicates that HFD suppresses BDNF/NTRK2 signal activation in the olfactory bulb, impairing serotonin neuronal function. The dopamine receptor DRD2 is predominantly expressed in the somata of mature olfactory sensory neurons [68]. The binding of dopamine to DRD2 suppresses cAMP signaling, influencing cell excitability in olfactory receptor neurons [69,70]. Our findings reveal that HFD upregulates the expression of Drd1 and Drd2 in the olfactory bulb, affecting dopaminergic neuronal function.

The reduction in CD14 expression in HFD-fed mice may potentiate the inflammatory response through the p38-MAPK pathway (Fig. 2B) [71]. Furthermore, CD105, identified as an endoglin, is associated with endothelial permeability [72], increased immune cell response [73], and increased microglial activation [74]. Our data illustrates that HFD intensifies the inflammatory response, immune response, and blood vessel endothelial permeability by elevating CD105 expression [75].

Moreover, the IGF family includes IGF-1, IGF-1 receptors, and IGF-binding proteins (IGFBPs), such as IGFBP-1 [76]. Insulin receptors [77,78] and IGFBPs [79] are abundant in the olfactory bulb among all brain regions. Insulin receptors are differently expressed in olfactory brain regions, such as the olfactory tubercule, piriform cortex, and olfactory nucleus [80]. The mitral cell layer shows the highest density of insulin receptors compared to granular cell and glomerular cell layers [81]. IGF-1 is found in olfactory endothelial cells and olfactory bulb [82] and promotes olfactory bulb maturation, cell proliferation of the olfactory endothelial cells [76,83,84],

Table 1
List of differentially expressed circRNAs in the olfactory bulb of mice fed normal and high-fat diet.

Locus	Host gene	Strand	Average (NFD)	Average (HFD)	Log2Fold	*p*-value	Exon counts
chr16:85013627–85030365	*APP*	–	7.4	3.4	−1.127	0.031	5
chr1:52708164-52709755	*MFSD6*	–	9.5	4.5	−1.093	0.010	1
chr17:86488160–86496111	*PRKCE*	+	16.2	8.2	−0.980	0.042	4
chr6:31418931-31433131	*MKLN1*	+	9.2	5.0	−0.872	0.007	5
chr2:158035996-158058827	*RPRD1B*	+	10.8	6.0	−0.843	0.013	5
chr2:140042094-140057499	*TASP1*	–	13.2	8.3	−0.662	0.034	3
chr16:97038898–97056765	*DSCAM*	–	13.6	9.3	−0.547	0.020	2
chr13:45852328–45956575	*ATXN1*	–	15.5	12.3	−0.338	0.045	2
chr18:79086551–79087180	*SETBP1*	–	18.3	24.9	0.449	0.031	1
chr16:94383912–94393174	*TTC3*	+	5.0	7.0	0.492	0.003	9
chr9:8634047-8658377	*TRPC6*	+	5.9	12.4	1.058	0.019	7
chr5:107788199-107799260	*EVI5*	–	3.7	8.0	1.108	0.036	5
chr6:84989325-85005036	*EXOC6B*	–	3.0	9.7	1.696	0.024	4

Table 2
List of PCR primer sequences used in this study.

Primer	Forward sequence	Reverse sequence
circAPP	TTGGCTTTCTGGAAATGGGC	GTTATGACACACCTCCGTGTG
circTrpc6	GAACTTCACTGCCATGGTCTG	CAGGAAGTCACGAAGACCTTTC
Ffar1	GTTTCATAAACCCGGACCTAGG	CATATTGTTCCCCGTCCAGG
Ffar4	TTTTGTGACTTTGAACTTCCTGG	GTTGGGACACTCGGATCTG
Pdk4	CCCGTTACCAATCAAAATCTTCAG	ACAGTTTGGGTCGATACTTCC
Irs2	ACTACCACAGTCCTACCTCAG	TCTTCAAGTCCAATCCCACG
Slc2a1	GATTGGTTCCTTCTCTGTCGG	CCCAGGATCAGCATCTCAAAG
Slc2a4	ACCCTCACTACGCTCTGG	CAACACGGCCAAGACATTG
Slc2a5	ATCACTGTCGGCATCCTTG	GCTCTCGGGAAAGAACGG
Ntrk2	GCCAACTATCACGTTTCTCGAG	CCATGGTACTCCGTGTGATTG
Scn1b	AGGAAGATGAGCGCTTTGAG	GAAGAGGAGACGGTAGACGT
Drd1	CTTCTGTGGCTCTGAGGAGAC	GGCATTATTCGTTGTAGGGCAG
Drd1	CTTCACCATCTCTTGCCCAC	GAGTGGTGTCTTCAGGTTGG
Gapdh	AATGTGTCCGTCGTGGATCT	AGACAACCTGGTCCTCAGTG

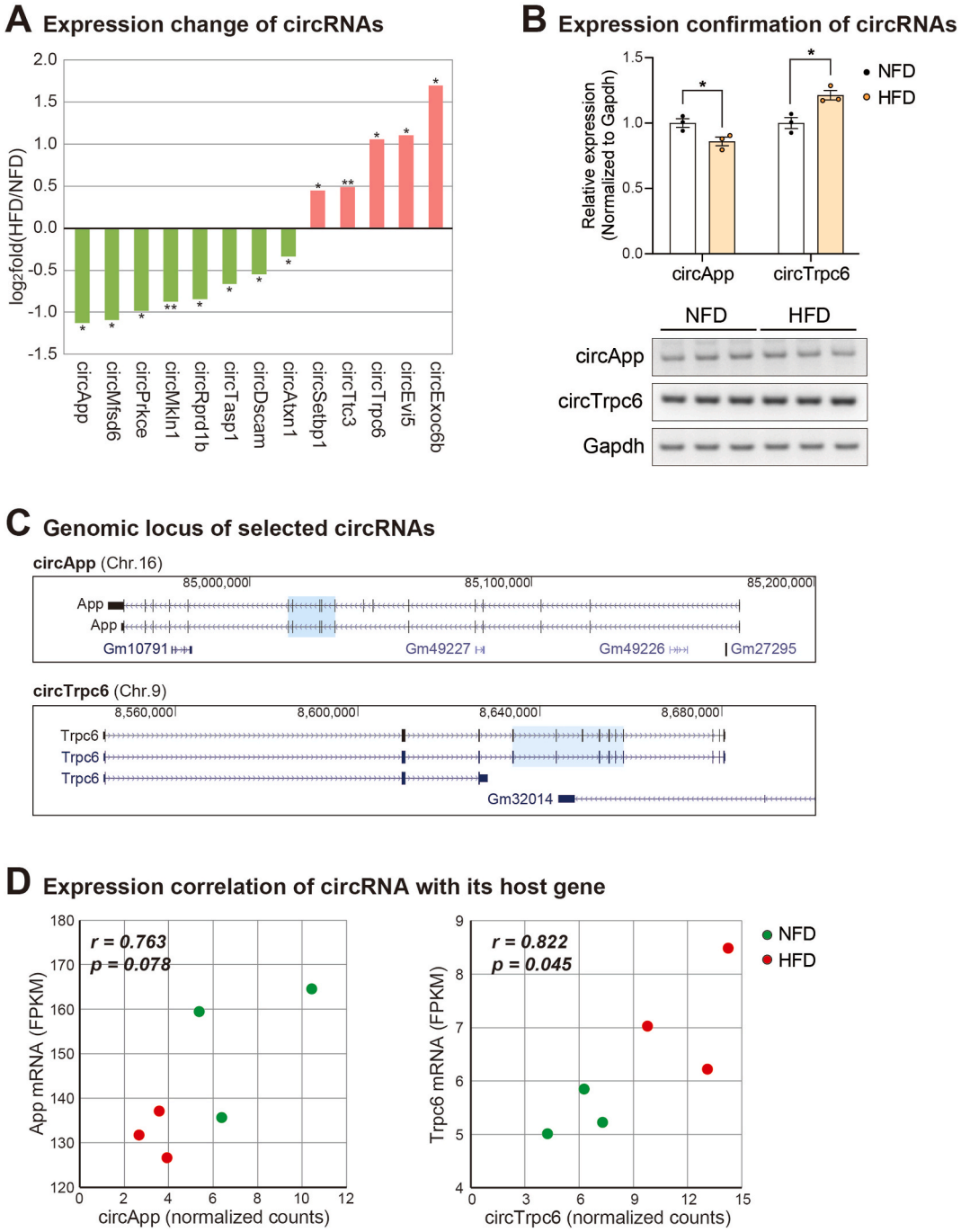

Fig. 4. Analysis of the expression changes of selected circular RNAs (circRNAs) and their relationship with their host genes. (A) Expression change of circRNAs. The expression differences in the olfactory bulb of normal-fat diet (NFD)-fed versus high-fat diet (HFD)-fed mice are presented (*$p < 0.05$, **$p < 0.01$) for the most significantly changed circRNAs ($p < 0.05$). (B) Expression confirmation of circRNAs. Confirmation of the expression of circApp and circTrpc6 in the olfactory bulb of NFD- and HFD-fed mice using real-time polymerase chain reaction (RT-PCR). circRNA expressions were normalized to *GAPDH*. Data are presented as the mean ± standard error of the mean (SEM; $n = 3$). Statistical analyses were performed using a one-sided Mann-Whitney *U* test (circApp: p = 0.05; circTrpc6: p = 0.05; *$p < 0.05$). (C) Genomic locus of selected circRNAs. The genomic positions of circApp and circTrpb6 are shown based on the information obtained from the UCSC Genome Browser (https://genome.ucsc.edu/). The exons used to produce circRNAs were highlighted with blue shadow. (D) Expression correlation of circRNA with host gene. These graphs show expression correlation between circAPP, circTrpb6 and its corresponding host mRNA. Green dots indicate the samples collected from NFD-fed mice, and red dots indicate those from HFD-fed mice. NFD: normal fat diet, HFD: high fat diet.

and neuronal differentiation and migration from the subventricular zone to the rostral migratory stream [85]. Based on previous findings, our findings indicate that HFD diminishes insulin sensitivity, olfactory bulb maturation, neurogenesis, and neuronal differentiation by reducing IGFBP-1. Furthermore, HFD induces leptin resistance and elevates plasma leptin levels, culminating in lipogenesis and inflammation [86,87]. Our data underscores that HFD amplifies leptin secretion, ultimately fostering inflammation and vascular dysfunction.

Given the GO analysis results related to increased genes (Fig. 1D), we anticipated that the biogenesis of diverse non-coding RNA types might be influenced, considering the enrichment of terms such as RNA binding and mRNA metabolic processing in the olfactory bulb of HFD-fed mice. Notably, miRNAs, as a non-coding RNA, contribute to pathological processes in the CNS [88,89]. Among the miRNAs produced from lncRNA loci, which were increased in the olfactory bulb of HFD-fed mice, miR-124 and miR-325 expression was changed in the olfactory bulb neurons due to HFD (Fig. 3C). miR-124 is the most enriched miRNA in the brain [90] that promotes neural stem cell proliferation, synapse plasticity, neurogenesis, and spine density of newborn olfactory bulb neurons [91,92]. Moreover, miR-325 is exclusively expressed in the brain of mice, suggesting its possible role in neuronal function [93].

Although App function has been extensively studied in the context of Alzheimer's disease and neural plasticity, its role in the normal function or development of the olfactory bulb is unknown. Our analysis showed that both App and circApp, an App-derived circRNA (Fig. 4D), were reduced in the olfactory bulb of HFD-fed mice. Because App is involved in synaptic function and neuronal growth and development, reduced App expression in the olfactory bulb of HFD-fed mice could influence neuronal function, as expected from the GO analysis results (Fig. 1C).

TRPC6, the host gene of circTrpb6 (Fig. 4D), was related to neurite outgrowth and BDNF-related signaling. In diet-induced obesity rats, *TRPC6* expression was upregulated in the hippocampus [94]. *TRPC6* is essential for BDNF-mediated nerve growth cone guidance, with *TRPC6* activation promoting neuronal migration [95]. Some studies reported that *TRPC6* boosts neuronal dendrite outgrowth through the CaMKIV-CREB-dependent pathway [96,97]. Another study reported that *TRPC6* is found both in the presynaptic and postsynaptic sites and contributes to excitatory synapse formation [98]. Our results showed that *TRPC6* and circTrpc6 expression was increased in the olfactory bulb of HFD-fed mice (Fig. 4D).

Our investigation revealed significant changes in the expression of both coding and non-coding RNAs, along with mRNAs, within the olfactory bulb of HFD-fed mice. Concurrently, multiple cytokine modifications were observed in the plasma of these mice. Therefore, altered cytokine patterns due to metabolic changes have a significant impact on the function of olfactory neurons, raising the possibility that metabolic disease may contribute to neurological impairment.

Compared to the previous study by Makhlouf et al. [19], which investigated the changes in highly expressed molecular signaling in the olfactory bulb and food choice following HFD, our research focuses on the specific changes in non-coding and protein-coding RNAs in the olfactory bulb after HFD. Makhlouf et al. found that two-month HFD feeding changed odor-guided behavior, mitochondrial biogenesis, and brain glucose metabolism. We examined genes directly related to olfactory function, including those involved in neurogenesis, synapse formation, and neuron projection, in mice fed a four-month HFD. Additionally, we identified candidate plasma inflammatory cytokines in these mice.

Although we identified the differential expression of diverse RNAs, we did not confirm whether the modulation of selected lncRNAs or circRNAs can improve odor behavior and odor-related cognitive performance in animals. Nevertheless, we suggest that the identification of diverse gene changes in this study underscores the potential value of future research endeavors focused on elucidating the intricate relationship between metabolic diseases and changes in the nervous system.

5. Conclusions

In conclusion, our findings demonstrate that the HFD alters the expression of several genes involved in neurogenesis, synaptic formation, free fatty acid metabolism, insulin signaling, and neurotransmitter regulation in the olfactory bulb. Additionally, HFD affects cytokine secretion patterns and alters the expression of specific lncRNAs, miRNAs, and circRNAs in the olfactory bulb. While our study provides novel insights into the genetic changes occurring in the olfactory bulbs of HFD-induced obese mice, there are certain limitations. Further functional studies are required to elucidate the roles and cellular mechanisms of the selected non-coding RNAs across different olfactory bulb cell types in the context of obesity. Moreover, animal behavioral studies are necessary to assess whether these genetic alterations influence olfactory function and olfactory-related memory. Consequently, our study establishes a foundational framework for the development of RNA-based therapies targeting olfactory dysfunction in obese individuals.

CRediT authorship contribution statement

Young-Kook Kim: Writing – original draft, Visualization, Validation, Methodology, Investigation, Funding acquisition, Formal analysis, Conceptualization. **Danbi Jo:** Writing – original draft, Visualization, Validation, Methodology, Investigation, Formal analysis, Data curation. **Seoyoon Choi:** Visualization, Validation, Methodology, Investigation. **Juhyun Song:** Writing – review & editing, Writing – original draft, Visualization, Validation, Supervision, Software, Resources, Project administration, Methodology, Investigation, Funding acquisition, Formal analysis, Data curation, Conceptualization.

Data availability

The raw RNA-seq data produced in this study was deposited in the Gene Expression Omnibus (GEO) with the accession number of GSE277760.

Declaration of competing interest

The authors declare no conflicts of interest.

Acknowledgments

This study was supported by grants RS-2022-NR069292 (Juhyun Song) and RS-2024-00333553 (Young-Kook Kim) from the National Research Foundation of Korea (NRF), Republic of Korea. Graphic abstract and Fig. 1A were created using BioRender (BioRender.com).

Appendix A. Supplementary data

Supplementary data to this article can be found online at https://doi.org/10.1016/j.heliyon.2025.e42196.

Gene abbreviations

IGF1	Insulin like growth factor 1
Fgf10	Fibroblast growth factor 10
Ecm1	Extracellular matrix protein 1
Nmnat2	Nicotinamide nucleotide adenylyltransferase 2
Ffar1	Free fatty acid receptor 1
Ffar4	Free fatty acid receptor 4
Pdk4	Pyruvate dehydrogenase kinase 4
Irs2	Insulin receptor substrate 2
Slc2a1	Solute carrier family 2 member 1
Slc2a4	Solute carrier family 2 member 4
Slc2a5	Solute carrier family 2 member 5
Ntrk2	Neurotrophic receptor tyrosine kinase 2
Scn1b	Sodium voltage-gated channel beta subunit 1
Drd1	Dopamine receptor D1
Drd2	Dopamine receptor D2
GABA	gamma-aminobutyric acid
CD14	Cluster of differentiation 14
EGF	Epidermal growth factor
IGFBP-1	Insulin-like growth factor-binding protein 1
MMP2	Matrix metalloproteinase-2
CD105	Endoglin
Dgcr8	DiGeorge syndrome critical region 8
Tarbp2	TARBP2 subunit of RISC loading complex
Trpc6	Transient receptor potential cation channel subfamily c member 6
App	Amyloid beta precursor protein
Dpf3	Double PHD fingers 3
Cops9	COP9 signalosome subunit 9
Bccip	BRCA2 and CDKN1A interacting protein
Ptov1	prostate tumor overexpressed gene 1
BDNF	Brain-derived neurotrophic factor
CD14	Cluster of differentiation 14
p38-MAPK	p38 mitogen-activated protein kinase

References

[1] H. Saito, H. Nishizumi, S. Suzuki, H. Matsumoto, N. Ieki, T. Abe, H. Kiyonari, M. Morita, H. Yokota, N. Hirayama, T. Yamazaki, T. Kikusui, K. Mori, H. Sakano, Immobility responses are induced by photoactivation of single glomerular species responsive to fox odour TMT, Nat. Commun. 8 (2017) 16011.
[2] R.L. Doty, Odor-guided behavior in mammals, Experientia 42 (1986) 257–271.
[3] J. Attems, L. Walker, K.A. Jellinger, Olfaction and aging: a Mini-review, Gerontology 61 (2015) 485–490.
[4] C. Linster, A. Fontanini, Functional neuromodulation of chemosensation in vertebrates, Curr. Opin. Neurobiol. 29 (2014) 82–87.
[5] N.E. Schoppa, N.N. Urban, Dendritic processing within olfactory bulb circuits, Trends Neurosci. 26 (2003) 501–506.
[6] G.U. Hoglinger, D. Alvarez-Fischer, O. Arias-Carrion, M. Djufri, A. Windolph, U. Keber, A. Borta, V. Ries, R.K. Schwarting, D. Scheller, W.H. Oertel, A new dopaminergic nigro-olfactory projection, Acta Neuropathol. 130 (2015) 333–348.
[7] M. Bendahmane, M.C. Ogg, M. Ennis, M.L. Fletcher, Increased olfactory bulb acetylcholine bi-directionally modulates glomerular odor sensitivity, Sci. Rep. 6 (2016) 25808.
[8] Z. Huang, N. Thiebaud, D.A. Fadool, Differential serotonergic modulation across the main and accessory olfactory bulbs, J. Physiol. 595 (2017) 3515–3533.
[9] R.M. Carey, M. Wachowiak, Effect of sniffing on the temporal structure of mitral/tufted cell output from the olfactory bulb, J. Neurosci. 31 (2011) 10615–10626.
[10] M.M. Misiak, M.S. Hipolito, H.W. Ressom, T.O. Obisesan, K.F. Manaye, E.A. Nwulia, Apo E4 alleles and impaired olfaction as predictors of alzheimer's disease, Clin Exp Psychol 3 (2017).
[11] R.B. Kay, E.A. Meyer, K.R. Illig, P.C. Brunjes, Spatial distribution of neural activity in the anterior olfactory nucleus evoked by odor and electrical stimulation, J. Comp. Neurol. 519 (2011) 277–289.
[12] J.A. Gottfried, Central mechanisms of odour object perception, Nat. Rev. Neurosci. 11 (2010) 628–641.
[13] R.L. Doty, S. Philip, K. Reddy, K.L. Kerr, Influences of antihypertensive and antihyperlipidemic drugs on the senses of taste and smell: a review, J. Hypertens. 21 (2003) 1805–1813.
[14] D.A. Fadool, K. Tucker, P. Pedarzani, Mitral cells of the olfactory bulb perform metabolic sensing and are disrupted by obesity at the level of the Kv1.3 ion channel, PLoS One 6 (2011) e24921.
[15] K. Tucker, S. Cho, N. Thiebaud, M.X. Henderson, D.A. Fadool, Glucose sensitivity of mouse olfactory bulb neurons is conveyed by a voltage-gated potassium channel, J. Physiol. 591 (2013) 2541–2561.
[16] M.E. Lean, D. Malkova, Altered gut and adipose tissue hormones in overweight and obese individuals: cause or consequence? Int. J. Obes. 40 (2016) 622–632.
[17] A.E. Durham, Insulin dysregulation and obesity: you are what you eat, Vet. J. 213 (2016) 90.
[18] Y.F. Brunner, C. Benedict, J. Freiherr, Intranasal insulin reduces olfactory sensitivity in normosmic humans, J. Clin. Endocrinol. Metab. 98 (2013) E1626–E1630.
[19] M. Makhlouf, D.G. Souza, S. Kurian, B. Bellaver, H. Ellis, A. Kuboki, A. Al-Naama, R. Hasnah, G.T. Venturin, J. Costa da Costa, N. Venugopal, D. Manoel, J. Mennella, J. Reisert, M.G. Tordoff, E.R. Zimmer, L.R. Saraiva, Short-term consumption of highly processed diets varying in macronutrient content impair the sense of smell and brain metabolism in mice, Mol. Metabol. 79 (2024) 101837.
[20] G. Lietzau, T. Nystrom, Z. Wang, V. Darsalia, C. Patrone, Western diet accelerates the impairment of odor-related learning and olfactory memory in the mouse, ACS Chem. Neurosci. 11 (2020) 3590–3602.
[21] G.J. Zou, J.Z. Su, Z.Q. Jiang, K.Z. Chen, Z.H. Zeng, L.X. Zhang, C.Q. Li, F. Li, Environmental enrichment ameliorates high-fat diet induced olfactory deficit and decrease of parvalbumin neurons in the olfactory bulb in mice, Brain Res. Bull. 179 (2022) 13–24.
[22] Y. Niu, P. Chang, T. Liu, X. Shen, H. Zhao, M. Zhang, S. Lei, B. Chen, J. Yu, Obese mice induced by high-fat diet have differential expression of circular RNAs involved in endoplasmic reticulum stress and neuronal synaptic plasticity of hippocampus leading to obesity-associated cognitive impairment, Front. Mol. Neurosci. 15 (2022) 1000482.
[23] C.E. Riera, A. Dillin, Emerging role of sensory perception in aging and metabolism, Trends Endocrinol. Metabol. 27 (2016) 294–303.
[24] C.E. Riera, E. Tsaousidou, J. Halloran, P. Follett, O. Hahn, M.M.A. Pereira, L.E. Ruud, J. Alber, K. Tharp, C.M. Anderson, H. Bronneke, B. Hampel, C.D.M. Filho, A. Stahl, J.C. Bruning, A. Dillin, The sense of smell impacts metabolic health and obesity, Cell Metabol. 26 (2017) 198–211, e195.
[25] W.H. Lee, J.H. Wee, D.K. Kim, C.S. Rhee, C.H. Lee, S. Ahn, J.H. Lee, Y.S. Cho, K.H. Lee, K.S. Kim, S.W. Kim, A. Lee, J.W. Kim, Prevalence of subjective olfactory dysfunction and its risk factors: Korean national health and nutrition examination survey, PLoS One 8 (2013) e62725.
[26] Z. Huang, S. Huang, H. Cong, Z. Li, J. Li, K.L. Keller, G.C. Shearer, P.M. Kris-Etherton, S. Wu, X. Gao, Smell and taste dysfunction is associated with higher serum total cholesterol concentrations in Chinese adults, J. Nutr. 147 (2017) 1546–1551.
[27] M. Faour, C. Magnan, H. Gurden, C. Martin, Olfaction in the context of obesity and diabetes: insights from animal models to humans, Neuropharmacology 206 (2022) 108923.
[28] Z. Zhang, B. Zhang, X. Wang, X. Zhang, Q.X. Yang, Z. Qing, W. Zhang, D. Zhu, Y. Bi, Olfactory dysfunction mediates adiposity in cognitive impairment of type 2 diabetes: insights from clinical and functional neuroimaging studies, Diabetes Care 42 (2019) 1274–1283.
[29] V. Precone, T. Beccari, L. Stuppia, M. Baglivo, S. Paolacci, E. Manara, G.A.D. Miggiano, B. Falsini, A. Trifiro, A. Zanlari, K.L. Herbst, V. Unfer, M. Bertelli, P. Geneob, Taste, olfactory and texture related genes and food choices: implications on health status, Eur. Rev. Med. Pharmacol. Sci. 23 (2019) 1305–1321.
[30] B.E. Richardson, E.A. Vander Woude, R. Sudan, J.S. Thompson, D.A. Leopold, Altered olfactory acuity in the morbidly obese, Obes. Surg. 14 (2004) 967–969.
[31] N. Thiebaud, M.C. Johnson, J.L. Butler, G.A. Bell, K.L. Ferguson, A.R. Fadool, J.C. Fadool, A.M. Gale, D.S. Gale, D.A. Fadool, Hyperlipidemic diet causes loss of olfactory sensory neurons, reduces olfactory discrimination, and disrupts odor-reversal learning, J. Neurosci. 34 (2014) 6970–6984.
[32] Y.K. Kim, RNA therapy: rich history, various applications and unlimited future prospects, Exp. Mol. Med. 54 (2022) 455–465.
[33] T.T. Rohn, D. Radin, T. Brandmeyer, P.G. Seidler, B.J. Linder, T. Lytle, J.L. Mee, F. Macciardi, Intranasal delivery of shRNA to knockdown the 5HT-2A receptor enhances memory and alleviates anxiety, Transl. Psychiatry 14 (2024) 154.
[34] J. Li, H. Peng, W. Zhang, M. Li, N. Wang, C. Peng, X. Zhang, Y. Li, Enhanced nose-to-brain delivery of combined small interfering RNAs using lesion-recognizing nanoparticles for the synergistic therapy of Alzheimer's disease, ACS Appl. Mater. Interfaces 15 (2023) 53177–53188.
[35] H. Goel, V. Kalra, S.K. Verma, S.K. Dubey, A.K. Tiwary, Convolutions in the rendition of nose to brain therapeutics from bench to bedside: feats & fallacies, J. Contr. Release 341 (2022) 782–811.
[36] C.V. Pardeshi, V.S. Belgamwar, Direct nose to brain drug delivery via integrated nerve pathways bypassing the blood-brain barrier: an excellent platform for brain targeting, Expet Opin. Drug Deliv. 10 (2013) 957–972.
[37] A.E. Aly, B.L. Waszczak, Intranasal gene delivery for treating Parkinson's disease: overcoming the blood-brain barrier, Expet Opin. Drug Deliv. 12 (2015) 1923–1941.
[38] O. Omotola, S. Legan, E. Slade, A. Adekunle, J.S. Pendergast, Estradiol regulates daily rhythms underlying diet-induced obesity in female mice, Am. J. Physiol. Endocrinol. Metab. 317 (2019) E1172–E1181.
[39] M. Varghese, C. Griffin, S. Abrishami, L. Eter, N. Lanzetta, L. Hak, J. Clemente, D. Agarwal, A. Lerner, M. Westerhoff, R. Patel, E. Bowers, M. Islam, P. Subbaiah, K. Singer, Sex hormones regulate metainflammation in diet-induced obesity in mice, J. Biol. Chem. 297 (2021) 101229.
[40] A.M. Bolger, M. Lohse, B. Usadel, Trimmomatic: a flexible trimmer for Illumina sequence data, Bioinformatics 30 (2014) 2114–2120.
[41] A. Dobin, C.A. Davis, F. Schlesinger, J. Drenkow, C. Zaleski, S. Jha, P. Batut, M. Chaisson, T.R. Gingeras, STAR: ultrafast universal RNA-seq aligner, Bioinformatics 29 (2013) 15–21.
[42] C. Trapnell, A. Roberts, L. Goff, G. Pertea, D. Kim, D.R. Kelley, H. Pimentel, S.L. Salzberg, J.L. Rinn, L. Pachter, Differential gene and transcript expression analysis of RNA-seq experiments with TopHat and Cufflinks, Nat. Protoc. 7 (2012) 562–578.
[43] J. Song, Y.K. Kim, Discovery and functional prediction of long non-coding RNAs common to ischemic stroke and myocardial infarction, J Lipid Atheroscler 9 (2020) 449–459.

[44] R. Patro, G. Duggal, M.I. Love, R.A. Irizarry, C. Kingsford, Salmon provides fast and bias-aware quantification of transcript expression, Nat. Methods 14 (2017) 417–419.
[45] M.D. Robinson, D.J. McCarthy, G.K. Smyth, edgeR: a Bioconductor package for differential expression analysis of digital gene expression data, Bioinformatics 26 (2010) 139–140.
[46] J. Cheng, F. Metge, C. Dieterich, Specific identification and quantification of circular RNAs from sequencing data, Bioinformatics 32 (2016) 1094–1096.
[47] A. Liberzon, A. Subramanian, R. Pinchback, H. Thorvaldsdottir, P. Tamayo, J.P. Mesirov, Molecular signatures database (MSigDB) 3.0, Bioinformatics 27 (2011) 1739–1740.
[48] H. Kristinsson, P. Bergsten, E. Sargsyan, Free fatty acid receptor 1 (FFAR1/GPR40) signaling affects insulin secretion by enhancing mitochondrial respiration during palmitate exposure, Biochim. Biophys. Acta 1853 (2015) 3248–3257.
[49] M. Duah, K. Zhang, Y. Liang, V.A. Ayarick, K. Xu, B. Pan, Immune regulation of poly unsaturated fatty acids and free fatty acid receptor 4, J. Nutr. Biochem. 112 (2023) 109222.
[50] J.J. Quinn, H.Y. Chang, Unique features of long non-coding RNA biogenesis and function, Nat. Rev. Genet. 17 (2016) 47–62.
[51] S. Haque, L.W. Harries, Circular RNAs (circRNAs) in health and disease, Genes 8 (2017).
[52] A. Gu, D.K. Jaijyan, S. Yang, M. Zeng, S. Pei, H. Zhu, Functions of circular RNA in human diseases and illnesses, Noncoding RNA 9 (2023).
[53] C. Deyts, M. Clutter, N. Pierce, P. Chakrabarty, T.B. Ladd, A. Goddi, A.M. Rosario, P. Cruz, K. Vetrivel, S.L. Wagner, G. Thinakaran, T.E. Golde, A.T. Parent, APP-mediated signaling prevents memory decline in Alzheimer's disease mouse model, Cell Rep. 27 (2019) 1345–1355, e1346.
[54] N. Zernov, A.V. Veselovsky, V.V. Poroikov, D. Melentieva, A. Bolshakova, E. Popugaeva, New positive TRPC6 modulator penetrates blood-brain barrier, eliminates synaptic deficiency and restores memory deficit in 5xFAD mice, Int. J. Mol. Sci. 23 (2022).
[55] X. Wu, W. Cao, C. Lu, L. Zuo, X. Liu, M. Qi, circ3323 motivates host gene to promote the aggressiveness of bladder cancer, Biochem. Genet. 60 (2022) 2327–2345.
[56] M.K. Hajihosseini, S. De Langhe, E. Lana-Elola, H. Morrison, N. Sparshott, R. Kelly, J. Sharpe, D. Rice, S. Bellusci, Localization and fate of Fgf10-expressing cells in the adult mouse brain implicate Fgf10 in control of neurogenesis, Mol. Cell. Neurosci. 37 (2008) 857–868.
[57] T. Goodman, S.G. Nayar, S. Clare, M. Mikolajczak, R. Rice, S. Mansour, S. Bellusci, M.K. Hajihosseini, Fibroblast growth factor 10 is a negative regulator of postnatal neurogenesis in the mouse hypothalamus, Development 147 (2020).
[58] L.B. Thomas, M.A. Gates, D.A. Steindler, Young neurons from the adult subependymal zone proliferate and migrate along an astrocyte, extracellular matrix-rich pathway, Glia 17 (1996) 1–14.
[59] S. Bovetti, Y.C. Hsieh, P. Bovolin, I. Perroteau, T. Kazunori, A.C. Puche, Blood vessels form a scaffold for neuroblast migration in the adult olfactory bulb, J. Neurosci. 27 (2007) 5976–5980.
[60] S. Milde, J. Gilley, M.P. Coleman, Axonal trafficking of NMNAT2 and its roles in axon growth and survival in vivo, BioArchitecture 3 (2013) 133–140.
[61] J. Gilley, M.P. Coleman, Endogenous Nmnat2 is an essential survival factor for maintenance of healthy axons, PLoS Biol. 8 (2010) e1000300.
[62] P.M. Lledo, A. Saghatelyan, Integrating new neurons into the adult olfactory bulb: joining the network, life-death decisions, and the effects of sensory experience, Trends Neurosci. 28 (2005) 248–254.
[63] B.M. Chelette, A.M. Loeven, D.N. Gatlin, D.R. Landi Conde, C.M. Huffstetler, M. Qi, D.A. Fadool, Consumption of dietary fat causes loss of olfactory sensory neurons and associated circuitry that is not mitigated by voluntary exercise in mice, J. Physiol. 600 (2022) 1473–1495.
[64] M.P. Sahu, Y. Pazos-Boubeta, C. Pajanoja, S. Rozov, P. Panula, E. Castren, Neurotrophin receptor Ntrk2b function in the maintenance of dopamine and serotonin neurons in zebrafish, Sci. Rep. 9 (2019) 2036.
[65] E. Castren, H. Antila, Neuronal plasticity and neurotrophic factors in drug responses, Mol. Psychiatr. 22 (2017) 1085–1095.
[66] J. Wook Koo, B. Labonte, O. Engmann, E.S. Calipari, B. Juarez, Z. Lorsch, J.J. Walsh, A.K. Friedman, J.T. Yorgason, M.H. Han, E.J. Nestler, Essential role of mesolimbic brain-derived neurotrophic factor in chronic social stress-induced depressive behaviors, Biol. Psychiatr. 80 (2016) 469–478.
[67] A.E. Autry, L.M. Monteggia, Brain-derived neurotrophic factor and neuropsychiatric disorders, Pharmacol. Rev. 64 (2012) 238–258.
[68] H.Q. Zhou, L.J. Zhuang, H.Q. Bao, S.J. Li, F.Y. Dai, P. Wang, Q. Li, D.M. Yin, Olfactory regulation by dopamine and DRD2 receptor in the nose, Proc. Natl. Acad. Sci. U. S. A. 119 (2022) e2118570119.
[69] G. Vargas, M.T. Lucero, Dopamine modulates inwardly rectifying hyperpolarization-activated current (Ih) in cultured rat olfactory receptor neurons, J. Neurophysiol. 81 (1999) 149–158.
[70] Y. Okada, T. Miyamoto, K. Toda, Dopamine modulates a voltage-gated calcium channel in rat olfactory receptor neurons, Brain Res. 968 (2003) 248–255.
[71] B. Sahay, R.L. Patsey, C.H. Eggers, J.C. Salazar, J.D. Radolf, T.J. Sellati, CD14 signaling restrains chronic inflammation through induction of p38-MAPK/SOCS-dependent tolerance, PLoS Pathog. 5 (2009) e1000687.
[72] E. Rossi, A. Kauskot, F. Saller, E. Frezza, S. Poirault-Chassac, A. Lokajczyk, P. Bourdoncle, B. Saubamea, P. Gaussem, M. Pericacho, R. Bobe, C. Bachelot-Loza, S. Pasquali, C. Bernabeu, D.M. Smadja, Endoglin is an endothelial housekeeper against inflammation: insight in ECFC-related permeability through LIMK/cofilin pathway, Int. J. Mol. Sci. 22 (2021).
[73] S.K. Meurer, R. Weiskirchen, Endoglin: an 'accessory' receptor regulating blood cell development and inflammation, Int. J. Mol. Sci. 21 (2020).
[74] D.G. Walker, L.F. Lue, T.G. Beach, I. Tooyama, Microglial phenotyping in neurodegenerative disease brains: identification of reactive microglia with an antibody to variant of CD105/endoglin, Cells (2019) 8.
[75] A. Borai, C. Livingstone, H. Zarif, G. Ferns, Serum insulin-like growth factor binding protein-1: an improvement over other simple indices of insulin sensitivity in the assessment of subjects with normal glucose tolerance, Ann. Clin. Biochem. 46 (2009) 109–113.
[76] A.I. Farbman, J.A. Buchholz, Transforming growth factor-alpha and other growth factors stimulate cell division in olfactory epithelium in vitro, J. Neurobiol. 30 (1996) 267–280.
[77] J.L. Marks, D. Porte Jr., W.L. Stahl, D.G. Baskin, Localization of insulin receptor mRNA in rat brain by in situ hybridization, Endocrinology 127 (1990) 3234–3236.
[78] W.A. Banks, A.J. Kastin, W. Pan, Uptake and degradation of blood-borne insulin by the olfactory bulb, Peptides 20 (1999) 373–378.
[79] V.C. Russo, S.R. Edmondson, F.A. Mercuri, C.R. Buchanan, G.A. Werther, Identification, localization, and regulation of insulin-like growth factor binding proteins and their messenger ribonucleic acids in the newborn rat olfactory bulb, Endocrinology 135 (1994) 1437–1446.
[80] J.M. Hill, M.A. Lesniak, C.B. Pert, J. Roth, Autoradiographic localization of insulin receptors in rat brain: prominence in olfactory and limbic areas, Neuroscience 17 (1986) 1127–1138.
[81] P. Aime, C. Hegoburu, T. Jaillard, C. Degletagne, S. Garcia, B. Messaoudi, M. Thevenet, A. Lorsignol, C. Duchamp, A.M. Mouly, A.K. Julliard, A physiological increase of insulin in the olfactory bulb decreases detection of a learned aversive odor and abolishes food odor-induced sniffing behavior in rats, PLoS One 7 (2012) e51227.
[82] T.K. Lee, B.H. Chen, J.C. Lee, M.C. Shin, J.H. Cho, H.A. Lee, J.H. Choi, I.K. Hwang, I.J. Kang, J.H. Ahn, J.H. Park, S.Y. Choi, M.H. Won, Age-dependent decreases in insulin-like growth factor-I and its receptor expressions in the gerbil olfactory bulb, Mol. Med. Rep. 17 (2018) 8161–8166.
[83] Y. Suzuki, M. Takeda, Expression of insulin-like growth factor family in the rat olfactory epithelium, Anat. Embryol. 205 (2002) 401–405.
[84] R. Ueha, K. Kondo, S. Ueha, T. Yamasoba, Dose-dependent effects of insulin-like growth factor 1 in the aged olfactory epithelium, Front. Aging Neurosci. 10 (2018) 385.
[85] A. Hurtado-Chong, M.J. Yusta-Boyo, E. Vergano-Vera, A. Bulfone, F. de Pablo, C. Vicario-Abejon, IGF-I promotes neuronal migration and positioning in the olfactory bulb and the exit of neuroblasts from the subventricular zone, Eur. J. Neurosci. 30 (2009) 742–755.
[86] B. Xue, Y. Yu, Z. Zhang, F. Guo, T.G. Beltz, R.L. Thunhorst, R.B. Felder, A.K. Johnson, Leptin mediates high-fat diet sensitization of angiotensin II-elicited hypertension by upregulating the brain renin-angiotensin system and inflammation, Hypertension 67 (2016) 970–976.
[87] C.E. Koch, C. Lowe, D. Pretz, J. Steger, L.M. Williams, A. Tups, High-fat diet induces leptin resistance in leptin-deficient mice, J. Neuroendocrinol. 26 (2014) 58–67.

[88] F. Pourrajab, M. Babaei Zarch, M. BaghiYazdi, S. Hekmatimoghaddam, M.R. Zare-Khormizi, MicroRNA-based system in stem cell reprogramming; differentiation/dedifferentiation, Int. J. Biochem. Cell Biol. 55 (2014) 318–328.
[89] Y. Sun, Z.M. Luo, X.M. Guo, D.F. Su, X. Liu, An updated role of microRNA-124 in central nervous system disorders: a review, Front. Cell. Neurosci. 9 (2015) 193.
[90] W.H. Zhang, L. Jiang, M. Li, J. Liu, MicroRNA-124: an emerging therapeutic target in central nervous system disorders, Exp. Brain Res. 241 (2023) 1215–1226.
[91] G. Li, S. Ling, MiR-124 promotes newborn olfactory bulb neuron dendritic morphogenesis and spine density, J. Mol. Neurosci. 61 (2017) 159–168.
[92] M. Akerblom, R. Sachdeva, I. Barde, S. Verp, B. Gentner, D. Trono, J. Jakobsson, MicroRNA-124 is a subventricular zone neuronal fate determinant, J. Neurosci. 32 (2012) 8879–8889.
[93] C.Y. Park, L.T. Jeker, K. Carver-Moore, A. Oh, H.J. Liu, R. Cameron, H. Richards, Z. Li, D. Adler, Y. Yoshinaga, M. Martinez, M. Nefadov, A.K. Abbas, A. Weiss, L. L. Lanier, P.J. de Jong, J.A. Bluestone, D. Srivastava, M.T. McManus, A resource for the conditional ablation of microRNAs in the mouse, Cell Rep. 1 (2012) 385–391.
[94] P. Roy, I. Martinelli, M. Moruzzi, F. Maggi, C. Amantini, M.V. Micioni Di Bonaventura, C. Cifani, F. Amenta, S.K. Tayebati, D. Tomassoni, Ion channels alterations in the forebrain of high-fat diet fed rats, Eur. J. Histochem. 65 (2021).
[95] Y. Li, Y.C. Jia, K. Cui, N. Li, Z.Y. Zheng, Y.Z. Wang, X.B. Yuan, Essential role of TRPC channels in the guidance of nerve growth cones by brain-derived neurotrophic factor, Nature 434 (2005) 894–898.
[96] Y. Tai, S. Feng, R. Ge, W. Du, X. Zhang, Z. He, Y. Wang, TRPC6 channels promote dendritic growth via the CaMKIV-CREB pathway, J. Cell Sci. 121 (2008) 2301–2307.
[97] H.T. Cline, Dendritic arbor development and synaptogenesis, Curr. Opin. Neurobiol. 11 (2001) 118–126.
[98] J. Zhou, W. Du, K. Zhou, Y. Tai, H. Yao, Y. Jia, Y. Ding, Y. Wang, Critical role of TRPC6 channels in the formation of excitatory synapses, Nat. Neurosci. 11 (2008) 741–743.